Research Square

Preprints are preliminary reports that have not undergone peer review.
They should not be considered conclusive, used to inform clinical practice,
or referenced by the media as validated information.

Ferumoxytol-Enhanced Whole-body and Limited Whole-body MRI for Characterization of Complex Vascular Anomalies

Sahana Rajesh
Nationwide Children's Hospital
Hrishi Kousik
Nationwide Children's Hospital
Lamya Atweh
Nationwide Children's Hospital
Rida Salman
Nationwide Children's Hospital
Bhuvana Setty
Nationwide Children's Hospital
Esteban Fernandez-Faith
Nationwide Children's Hospital
Gregory Pearson
Nationwide Children's Hospital
Catherine Cottrell
Nationwide Children's Hospital
Anna P. Lillis
Akron Children's Hospital
Rajesh Krishnamurthy
rajesh.krishnamurthy@nationwidechildrens.org
Nationwide Children's Hospital

Research Article

Keywords:

Posted Date: August 12th, 2026

DOI: https://doi.org/10.21203/rs.3.rs-10462024/v1

License: This work is licensed under a Creative Commons Attribution 4.0 International License.
Read Full License

Additional Declarations: No competing interests reported.

Abstract

Background

Complex vascular anomalies (CVA) involve multiple tissue types across large anatomic regions, making characterization with conventional MRI challenging and time intensive. Whole-body (WB) or limited WB-MRI may enable more efficient assessment.

Objective

To retrospectively evaluate an abbreviated WB-MRI protocol using Ferumoxytol for comprehensive characterization of CVA.

Methods

Clinical, imaging and management information from patients undergoing Ferumoxytol-enhanced WB-MRI (July 2020-May 2025) was retrospectively reviewed following IRB approval. In the development phase, sequences tested included 3D-RAVE, 3D-VIBE, axial SSFSE T2, and 3D-T2-SPACE. Scan duration, technical image quality, and clinical grading of reporting elements for CVA were assessed by 2 radiologists. An abbreviated protocol was implemented using 3D-VIBE or RAVE, and axial SSFSE T2, with an optional time-resolved MRA using gadolinium contrast for high-flow lesions. Descriptive statistics and 2-tailed t-tests were utilized for analysis.

Results

Protocol development phase included 32 patients (15M,17F) median age 11.8y (0.2–52.4), and scan duration 57 min (17–134). Implementation phase involved 45 patients (17M, 28F) median age 10.6y (0.01–42.3), and scan duration 32 min (9–77). Average number of stations were RAVE (2.4), VIBE (4.3), SSFSE (3.6) and 3DT2 (2.6). Average technical image quality score was 4.3/5. Mean clinical grade of reporting elements was 4.6/5. Additional TWIST sequence was used in 5 patients to assess suspected high-flow component. All studies were diagnostic, with 3D VIBE/RAVE and SSFSE T2 mandatory for assessment. After multidisciplinary discussion, management decisions were altered in 57% of cases.

Conclusions

We demonstrate feasibility of an abbreviated WB MRI protocol using Ferumoxytol contrast for CVA.

Introduction

Vascular anomalies (VA) are classified into vascular tumors and vascular malformations (VMs) based on a binary classification scheme initially proposed in 1982 by Mulliken and Glowacki [1], which has since been regularly updated by the International Society for the Study of Vascular Anomalies (ISSVA) [2].

Vascular malformations are further divided by vessel type into simple (capillary, lymphatic, venous and arteriovenous malformations), combined (involving more than one type of blood vessel) and complex (characterized by segmental or whole-body involvement, tissue overgrowth, and involvement of other organ systems) [2]. Complex vascular anomalies (CVA) often have distinct histology and genetic drivers essential to establishing a definitive diagnosis: for instance, RAS/MEK/ERK pathway mutations (RASopathy) [3] are typically associated with high-flow lesions, while PIK3CA/Akt/mTOR pathway mutations are linked to slow-flow venous malformations [4]. These features are incorporated into the ISSVA classification and can further guide advanced imaging [5].

While the MRI protocol is well established in simple or combined high-flow or slow-flow lesions using a combination of T1, T2 and post-contrast T1 imaging augmented with time-resolved MRA [6], MRI is challenging with diffuse and/or complex malformations [7]. Diffuse VA frequently involve large anatomic regions—an entire extremity, one side/half of the body, or the brain, spine, and body. Complex malformations associated with PTEN Hamartoma Tumor Syndrome (PHTS) [8] and PIK3CA-related overgrowth syndromes (PROS) [9] represent a subset of these lesions. These malformations can combine high-flow and slow-flow vascular components or include overlapping slow-flow anomalies such as capillary-veno-lymphatic malformations, which complicates imaging protocol decisions about coverage, spatiotemporal resolution, and tissue characterization. Clinical presentation also varies widely, ranging from isolated digit enlargement to segmental overgrowth across multiple anatomic regions. Because these malformations often affect fat, muscle, vasculature, and bone, MRI must characterize both vascular and nonvascular tissue components comprehensively. As a result, imaging protocols are lengthy, requiring multiple sequences and stations to ensure tissue characterization and coverage.

The natural history of diffuse and complex VA is punctuated by complications related to the disease or its treatment, such as thrombosis, hemorrhage, contractures, end-organ changes, or non-target embolism, which can increase the risk of misdiagnosis, particularly outside of specialized multidisciplinary settings [10]. Even with specialist referral, the full extent of the VA is frequently underestimated, and syndromic involvement may be mischaracterized or only partially recognized—due in part to the limitations of conventional MRI protocols, which are often incapable of delivering efficient, whole-body coverage.

Two recent advances may improve imaging efficiency for complex VA. First, whole-body (WB) or limited WB MRI (which uses multiple stations to cover large anatomical regions, but not head-toe) is increasingly used for surveillance of malignancy and genetic cancer-predisposition syndromes [11, 12]. Second, Ferumoxytol—a nanoparticle iron agent is a blood-pool contrast agent that uniformly fills all vascular channels, enabling rapid high-resolution 3D imaging of large regions with less need for sedation

[13]. Although considered off-label by the FDA for MRI, its safety profile in children and adults is well established [14, 15].

As part of a quality initiative to improve imaging experience for our burgeoning referral population of complex vascular anomalies, we developed an abbreviated protocol with Ferumoxytol contrast and evaluated the performance of several WB sequences in characterizing these lesions. Therefore, the objective for this study is to retrospectively evaluate our experience with an abbreviated, whole-body or limited whole body MR imaging protocol using Ferumoxytol blood-pool contrast agent to characterize complex vascular anomalies.

Materials and Methods

Study Design

Following IRB approval, we retrospectively identified patients who underwent imaging under an institutional clinical development protocol using Ferumoxytol-enhanced WB or limited WB MRI for evaluation of complex VA. At our institution, imaging approaches to support programmatic gowth of multidisciplinary specialist referral pathways like CVA are governed by a quality improvement approach. As part of such an approach, we developed an MRI protocol with Ferumoxytol contrast and evaluated the performance of several WB sequences in characterizing these lesions. Based on this assessment, an abbreviated protocol was implemented in our patients. A total of 77 patients were included: 32 during protocol development and 45 in the protocol implementation phase. Protocol development occurred from July 2020 to February 2022, with implementation data included from March 2022 up to May 2025, with no exclusion criteria and participants forming a consecutive series.

Referral Pathway

Most patients were referred through our institutional multidisciplinary Vascular Anomalies Clinic (VAC), which includes experts from interventional radiology, hematology-oncology, dermatology, and plastic surgery. Suspected diffuse lymphatic channel or lymphatic conduction anomalies were excluded in this series, due to the presence of a separate institutional pathway for MR lymphangiography and related interventions. Referral indications for the WB or limited WB imaging protocol were assessed, including screening for prior diagnosis of a syndromic or genetic VA, leg length discrepancy, or diffuse overgrowth, varicosities, edema or capillary stain. Clinical photographs, physical examination findings, and prior imaging were reviewed. When possible, targeted ultrasound performed by an interventional radiologist was used to assess the lesion extent and screen for high-flow components. Most cases were reviewed at the VAC, and a provisional complex VA diagnosis was assigned. Patients with concern for overgrowth, syndromic or diffuse anomalies are referred for WB MRI. A small number of patients were independently evaluated and referred from other services. After imaging and genetic testing (if applicable) was

completed, a revised diagnosis was rendered by the VAC or by the referring clinical team where indicated.

Data Collection

Clinical and imaging data were extracted from the electronic health records of all 77 patients. Demographic information included age at the time of scan, sex, and weight. Clinical context variables included the referring clinical service, referral diagnosis for WB imaging, and post-imaging diagnoses assigned by the VAC or referring clinical team.

Scan-related parameters included scan coverage (whether the scan was WB or limited WB), total scan duration, the number and type of sequences acquired, the number of stations used per sequence, anatomic regions covered, MRI procedure codes, contrast type/dose administered, and whether a composite whole-body image was generated during post-processing.

Imaging Protocol

MRI was performed on a 3T Siemens scanner (Prisma or Skyra, Siemens Healthineers, Forchheim, Germany) after slow intravenous infusion of Ferumoxytol (Feraheme, AMAG Pharmaceuticals; generic: Sandoz) according to our previously published institutional protocol [15]. All patients in this study were distinct from those included in the previously published cohort. During the development phase, four core MRI sequences and two optional sequences were used, with image grading limited to the core sequences (Table 1, Figs. 1–3). Stacks from the images were stitched to provide a composite dataset, which could be manipulated on a 3D workstation to obtain arbitrary planes (Figs. 2–4).

Table 1
MRI Sequences Used During Development Phase with Technical Image Grading

Sequence	Core or Optional	No of Patients in Dev. Phase	Relevant Scan Parameters	Rationale	Technical Image Quality Score
Axial single shot FSE T2-weighted imaging (SSFSE T2) without fat saturation	Core	28	Slice thickness: 3–5 mm, TE 120 ms, free breathing, breath-held or respiratory trig. in chest/abd only. 1–2 min per station	Main sequence for fluid sensitive imaging for LM, edema, soft tissue, viscera. Less signal to noise compared to 3D T2.	4.81 (4–5)
Volumetric Interpolated Breath-Hold Examination (VIBE)	Core	15	Breath-held in chest/abd, free-breathing in pelvis/extremities 1-1.5 mm isotropic resolution. 1–2 min per station	Main sequence for arterial, venous and soft tissue assessment.	4.21 (3–5)
Free-breathing radial volumetric encoding (RAVE)	Core	23	Free breathing, 1-1.5 mm isotropic resolution. 3–5 min per station.	Free breathing alternative to VIBE in smaller, non-cooperative patients	4.5 (2–5)
3D TSE T2-weighted Sampling Perfection with Application optimized Contrast (SPACE)	Core	20	Free breathing with respiratory triggering, 1-1.5 mm isotropic resolution, 5–7 min per station	Hi-resolution, fat suppressed 3D T2 weighted imaging, provides redundant info to SSFSE T2, prone to artifact.	4.07 (2–5)
ECG-gated and navigator respiratory-gated 3D GRE with inversion recovery-prepared fat suppression (3D IR-FLASH)	Optional	21	1-1.5 mm isotropic resolution, 50% nav efficiency, 5–7 min per station	For enhanced motion control in cardiac and abdominal imaging, if fine detail desired.	N/A
Time-resolved MRA with interleaved stochastic trajectories	Optional	1	1-1.5 mm isotropic resolution, 1–2 second dynamics, GRAPPA factor 4	Add-on for suspected high-flow component.	N/A

LM – lymphatic malformation, GRAPPA – Generalized Autocalibrating Partially Parallel Acquisitions

Sequence	Core or Optional	No of Patients in Dev. Phase	Relevant Scan Parameters	Rationale	Technical Image Quality Score
(TWIST) using Gad -based contrast					

LM – lymphatic malformation, GRAPPA – Generalized Autocalibrating Partially Parallel Acquisitions

The finalized abbreviated protocol used during the implementation phase included axial **SSFSE T2 (a**xial Single Shot FSE T2-weighted imaging) and 3D VIBE (Volumetric Interpolated Breath-Hold Examination) sequences, or 3D RAVE (Free-breathing radial volumetric encoding) for non-cooperative patients for motion compensation, with an optional high temporal resolution TWIST (Time-resolved MRA with Interleaved Stochastic Trajectories) sequence, with 1–2 second temporal resolution, used for suspected high-flow lesions (Figs. 5–6) .

Structured Image Interpretation

A standardized reporting template was created as part of this study to evaluate complex VA **(**Table 2**)**. The imaging report summarized the type of VA, its anatomical region, extent, critical relationships, extravascular involvement, and potential syndromic or genetic associations. The post-imaging follow-up VAC visit integrated MRI findings with relevant clinical, laboratory, genetic and ultrasound data, and served as a key driver of therapeutic decision-making based on multidisciplinary discussion.

Table 2
Reporting Template for Complex Vascular Anomalies and Clinical Grading of Vascular, and Extravascular Reporting Elements

Category	Reporting Element	Sequences	Score	Comment
Arterial	Arterial anatomy and arteriovenous (AV) shunting	VIBE / RAVE / Time resolved MRA if available	4.48 (3–5)	VIBE adequate for arterial integrity. Tr-MRA for AV shunting.
Venous	Deep venous system	VIBE / RAVE	4.67 (3–5)	Deep vein integrity assessment critical in KTS/ PROS.
	Superficial venous system	VIBE / RAVE	4.70 (3–5)	Distinguish varicosities due to VA from venous thrombosis / insufficiency.
	Anomalous veins	VIBE / RAVE	4.67 (3–5)	Common in KTS/ PROS.
	Superficial venous malformation	VIBE / RAVE	4.70 (3–5)	3D volume rendering useful for visualization.
	Deep/intramuscular VM	VIBE / RAVE	4.80 (4–5)	3D volume rendering useful for visualization. Potential for compartment syndrome after sclerotherapy.
Lymphatic	Macrocystic LM	SSFSE T2	4.74 (4–5)	Screen for isolated visceral involvement, quantify response to sclerotherapy.
		3D T2 SPACE	4.50 (3–5)	
	Microcystic LM	SSFSE T2	4.67 (4–5)	Adequate resolution needed to distinguish microcysts from edema.
		3D T2 SPACE	4.53 (3–5)	
	Soft tissue edema	SSFSE T2	4.63 (4–5)	Edema is non-specific, common, and rarely sign of lymphangiectasia or abnormal lymph conduction in this setting.
		3D T2 SPACE	4.38 (3–5)	
Overgrowth	Limb length discrepancy (LLD)	VIBE / RAVE	4.72 (4–5)	3D MR qualitative and not validated for LLD, use scanogram.

VIBE – Volumetric Interpolated Breath–Hold Examination, RAVE – Free–breathing Radial Volumetric Encoding, KTS – Klippel Trenaunay Syndrome, PROS – PIK3CA Related Overgrowth Syndrome, VM – Vascular Malformation, LM – Lymphatic Malformation, SSFSE T2 – Axial single shot FSE T2–weighted imaging, 3D T2 SPACE – 3D TSE T2–weighted Sampling Perfection with Application optimized Contrast, VA – vascular anomalies

Category	Reporting Element	Sequences	Score	Comment
	Focal fatty/soft tissue hypertrophy	VIBE / RAVE	4.77 (3–5)	MR highly sensitive, use perimeter comparison to contralateral side for soft tissue and extremity girth.
	Limb shape	VIBE / RAVE	4.75 (3–5)	3D volume rendering useful for identifying characteristic changes.
Other	Spine involvement	VIBE / RAVE / SSFSE T2	4.54 (3–5)	Any abnormality is indication for further dedicated spine imaging.
	Visceral organ involvement	VIBE / RAVE / SSFSE T2	4.70 (4–5)	Abdominal organs, gut involved in diffuse LM, VM.
	Bone/joint involvement	VIBE / RAVE / SSFSE T2	4.76 (3–5)	Common cause of functional impairment in VA. Bone infarcts common association.

VIBE – Volumetric Interpolated Breath–Hold Examination, RAVE – Free–breathing Radial Volumetric Encoding, KTS – Klippel Trenaunay Syndrome, PROS – PIK3CA Related Overgrowth Syndrome, VM – Vascular Malformation, LM – Lymphatic Malformation, SSFSE T2 – Axial single shot FSE T2–weighted imaging, 3D T2 SPACE – 3D TSE T2–weighted Sampling Perfection with Application optimized Contrast, VA – vascular anomalies

Technical and Clinical Grading

Two radiologists with 20 and 10 years of experience in pediatric vascular anomalies, respectively, evaluated technical image quality for the core sequences (SSFSE T2, RAVE, VIBE, 3D T2 SPACE (3D TSE T2-weighted Sampling Perfection with Application optimized Contrast)). Additionally, reporting elements relevant to vascular anomalies were graded. The radiologists used a consensus approach with a standardized Likert scale (1 = non-diagnostic; 5 = excellent) described previously [16].

Data Analysis

Descriptive statistics were used to analyze data. Continuous variables were summarized with means and ranges while frequencies and/or percentages were used for categorical variables. T-tests were used to compare scan duration and Ferumoxytol dosage between the development and implementation phases.

Results

Patient Characteristics

A total of 32 patients (15 males, 17 females) underwent imaging using the diffuse vascular malformation protocol during the development phase. The median age at scan was 11.8 years (range: 0.2–52.4 years), and the median weight was 42.6 kg (range: 4.7-156.8 kg). Nineteen patients (59%) had

prior MRIs performed either at our institution or an outside center, and 31 (97%) had prior review by a VAC specialist. WB MRI was performed in 4 patients during this phase, with the remainder undergoing limited WB imaging.

In the implementation phase, 47 patients (19 males, 28 females) were imaged with a median age of 10.6 years (range: 0.01–42.3 years) and a median weight of 46.4 kg (range: 3.6–111.4 kg).

Seventeen patients (36%) had prior MRIs performed either at our institution or an outside center, and 35 (75%) had prior review by a VAC specialist. WB MRI was performed in 4 patients and limited WB imaging in the rest.

Imaging Coverage and Order Codes

Imaging coverage in the development phase was from the pelvis to the toes (n = 14), followed by abdomen to toes (n = 5), brain to toes (n = 4), chest to fingers (n = 2), neck to fingers (n = 2), and one case each of the following ranges: neck to abdomen, neck to chest, brain to fingers, chest to toes, and chest to ankles. The most frequently used MRI order codes were MRA Extremity (n = 39), MRA Pelvis (n = 26), MRA Abdomen (n = 12), MRA Chest (n = 7), MR Head/Neck (n = 9).

Imaging coverage in the implementation phase was from the pelvis to the toes (n = 14), followed by brain to pelvis (n = 6), abdomen to toes (n = 5), neck to pelvis (n = 5), brain to toes (n = 4), abdomen to pelvis (n = 4), neck to abdomen (n = 3), neck to toes (n = 2), chest to pelvis (n = 2), and one case each of brain to abdomen and abdomen to ankles. The most frequently used MRI order codes were MRA Extremity (n = 39), MRA Pelvis (n = 37), MRA Abdomen (n = 24), MRA Chest (n = 22), MR Head/Neck (n = 19).

Imaging Protocol Utilization

During the development phase, core MRI sequences were performed in almost all patients, while optional sequences were utilized with varying frequency. The number of stations was determined by patient size and coverage needs. Utilization of core sequences was as follows: SSFSE T2 sequence was most used (28 times) with an average of 3.5 stations, followed by RAVE (23 uses, 2.3 stations), 3D T2 SPACE (20 uses, 2.5 stations), VIBE (15 uses, 3.6 stations). Optional sequence use included FLASH (Fast low angle shot MRA) (8 uses, 1.9 stations), and TWIST (2 uses with 24 dynamics). In the implementation phase, core sequences were VIBE (45 times, 2.9 stations) and SSFSE T2 (44 uses, 3.3 stations). Depending on coverage needs and indication, optional sequences included FLASH (14 uses, 1.3 stations), RAVE (5 uses, average 1.2 stations), 3D T2 SPACE (4 uses, average 2.0 stations), and TWIST (3 uses, mean 11.5 dynamics).

Scan Duration

The average scan duration significantly ($p < 0.001$) decreased from the development to the implementation phase. During development, the mean scan time was 57 minutes (range: 17–134 minutes), whereas in the implementation phase, the average protocol completion time was 32 minutes (range: 9–77 minutes).

Technical Grading

Technical image quality assessments were performed on all 32 patients studied during the development phase. Consensus scores for core sequences were high with an average technical image quality score of 4.3/5 as shown in Table 1.

Clinical Grading

Clinical image quality assessments were performed on all 32 patients studied during the development phase with results in Table 2. Mean clinical grade of reporting elements in VA was 4.6/5. Following Ferumoxytol administration, T2-weighted imaging effectively suppressed vascular signal, facilitating improved visualization of lymphatic components and soft tissue edema (Figs. 1–2). Additionally, SSFSE T2 and 3D T2 SPACE performed similarly in assessment of lymphatic components, obviating the need for performance of the time intensive 3D-T2 in the implementation phase (Fig. 1).

Referral Indications and Post-imaging follow-up

Referrals for MRI came from various VAC specialists. In the development phase, the most common referring specialties were interventional radiology (n = 11), hematology/oncology (n = 10), and plastic surgery (n = 5), clinical genetics (n = 3) and dermatology (n = 2). In the implementation phase, the distribution was similar with referrals from hematology/oncology (n = 15), interventional radiology (n = 10), plastic surgery (n = 5), and dermatology (n = 5).

Indications for imaging with the WB protocol included prior diagnosis of a syndromic or genetic VA, leg length discrepancy, or diffuse overgrowth/varicosities/edema/capillary stain. After multidisciplinary discussion, imaging diagnoses using the VAC WB protocol modified the initial VAC diagnoses and/or management 16/28 times (57%) during the development phase, and 12/24 times (50%) during the implementation phase (Table 3). PIK3CA spectrum of lesions were the most prevalent in our series with specific diagnoses of PROS (Figs. 1–3), KTS (Klippel-Trénaunay syndrome) (Fig. 2), CLOVES (Congenital lipomatous (fatty) overgrowth, vascular malformations, epidermal nevi and scoliosis/skeletal/spinal anomalies) (Fig. 4) or diffuse VM/VLM (vascular malformation/veno-lymphatic malformation) made after imaging in patients referred for overgrowth, varicosities or cutaneous changes being the most common scenario.

Table 3
Comparison of Pre-imaging VAC Diagnoses and Post-Imaging VAC/ Final Clinical Diagnoses

Development Phase		
	Pre-imaging VAC / referral dx	**Post-imaging VAC/ Final Clinical dx**
Diffuse VM	12	8
PIK3CA Related Overgrowth Syndrome	1	7
KTS	5	4
Overgrowth/hemihypertrophy	3	1
Capillary malformation / port wine stain	3	—
CLOVES	1	2
Diffuse LM	1	2
HHT	1	1
AVM	1	—
Suspected RASopathy	—	1
Hemangioma	—	1
Tuberous Sclerosis	—	1
Perforator incompetence with varicosities	—	1
Lymphedema	2	1
CMTC	—	1
Other	2	1
Implementation Phase		
Diffuse VM	9	3
PIK3CA Related Overgrowth Syndrome	4	8
Overgrowth / Hemihypertrophy	3	—

VM – vascular malformation, VAC – Vascular Anomalies Clinic, PIK3CA – Phosphatidylinositol–4,5–bisphosphate 3–kinase catalytic subunit alpha, KTS – Klippel Trenaunay Syndrome, LM – lymphatic malformation, VLM – veno–lymphatic malformation, CLOVES – congenital lipomatous (fatty) overgrowth, vascular malformations, epidermal nevi and scoliosis/skeletal/spinal anomalies, HHT – Hereditary Hemorrhagic Telangiectasia, AVM – arteriovenous malformation, CMTC – Cutis Marmorata Telangiectatica Congenita, LUMBAR Syndrome – Lower body hemangioma, Urogenital abnormalities/ulceration, Myelopathy of the spinal cord, Bony deformities, Anorectal malformations and arterial anomalies, Renal anomalies

Development Phase		
	Pre-imaging VAC / referral dx	**Post-imaging VAC/ Final Clinical dx**
KTS	3	4
Diffuse LM/VLM	2	3
CLOVES	—	1
HHT / Family history of HHT	9	6
AVM	1	1
Parkes Weber Syndrome	—	1
Capillary malfmn / port wine stain / cutaneous	8	—
Venous incompetence with varicosities	1	3
CMTC	—	1
Intestinal vascular malformation	1	—
Juvenile polyposis	—	1
Infantile segmental hemangioma	1	—
LUMBAR Syndrome	—	1
Normal vasculature	3	12

VM – vascular malformation, VAC – Vascular Anomalies Clinic, PIK3CA – Phosphatidylinositol–4,5–bisphosphate 3–kinase catalytic subunit alpha, KTS – Klippel Trenaunay Syndrome, LM – lymphatic malformation, VLM – veno–lymphatic malformation, CLOVES – congenital lipomatous (fatty) overgrowth, vascular malformations, epidermal nevi and scoliosis/skeletal/spinal anomalies, HHT – Hereditary Hemorrhagic Telangiectasia, AVM – arteriovenous malformation, CMTC – Cutis Marmorata Telangiectatica Congenita, LUMBAR Syndrome – Lower body hemangioma, Urogenital abnormalities/ulceration, Myelopathy of the spinal cord, Bony deformities, Anorectal malformations and arterial anomalies, Renal anomalies

Ferumoxytol dosing and dual contrast usage in suspected high-flow lesions

Ferumoxytol dosage showed a significant ($p < 0.001$) reduction between the development and implementation phases, reflecting increasing institutional experience with the drug and understanding of dose-related contrast in different age groups. The average dose administered during the development phase was 2.35 mg/kg (range: 1.0-3.5 mg/kg), compared to 1.93 mg/kg (range: 1.0-3.1 mg/kg) in the implementation phase. No adverse reactions were observed.

Five patients with suspected high-flow anomalies also had an additional high temporal resolution time resolved MRA sequence with a TWIST technique and received an average of 2.03 mg/kg of Ferumoxytol

followed by 0.12 mL/kg of gadobutrol (Gadavist) contrast (Table 4) without incident. All TWIST studies were graded as providing good arterial enhancement and reliable assessment for arteriovenous shunting (Figs. 5–6).

Table 4
Patients receiving dual contrast agents (Ferumoxytol and Gadavist) for suspected high flow component

Patient	Age (years)	Coverage	Referring Diagnosis	Post Imaging Diagnosis
1	12.1	Brain to pelvis	HHT	HHT
2	38.5	Chest and Right upper extremity	UE AVM	Multiple upper extremity AVMs with suspected RASopathy
3	0.1	Neck to pelvis	Intrahepatic AVM seen on fetal imaging	Normal
4	1.2	Chest to pelvis	N/A	Juvenile polyposis
5	0.2	Abdomen to toes	Segmental infantile hemangioma	LUMBAR Syndrome

HHT – Hereditary Hemorrhagic Telangiectasia, UE AVM – upper extremity arteriovenous malformation, AVM – arteriovenous malformation, LUMBAR Syndrome – Lower body hemangioma, Urogenital abnormalities/ulceration, Myelopathy of the spinal cord, Bony deformities, Anorectal malformations and arterial anomalies, Renal anomalies

Discussion

This study demonstrated the feasibility of a novel protocol utilizing ferumoxytol-enhanced WB MRI for assessing complex vascular malformations. We propose a final 30-minute ferumoxytol-enhanced protocol using 2 WB sequences—axial SSFSE T2 and 3D T1-VIBE—with an additional localized time-resolved MRA sequence when a high-flow component is present. This abbreviated protocol effectively delineated malformation type, anatomical region, extent, critical relationships, and extravascular involvement. A standardized template also supported follow-up assessment of treatment response.

Conventional MR sequences with ferumoxytol, and their adaptation for pediatric vascular anomalies, remain underexplored, and these data help address that gap. By creating a uniform dark-blood effect on T2-weighted sequences, this approach improves detection of microcystic and macrocystic lymphatic malformations (LM) in soft tissue and helps distinguish them from edema without need for fat suppression (Figs. 1–2). VIBE/RAVE sequences provide exquisite sensitivity for defining the extent of multiplanar venous involvement (Fig. 3), while high-resolution 3D acquisition captures soft tissue, bony, and articular involvement (Figs. 4–6). The main advantage of this protocol is that it simplifies screening and diagnosis for complex anomalies into a short, free-breathing, two-sequence exam that can be performed without supervision in non-specialized centers. Combined with the structured reporting template used in this study that targets vascular and non-vascular manifestations, broader adoption may

help standardize image acquisition and reporting across this diverse and challenging group of conditions.

Integrated with clinical, laboratory, genetic, and ultrasound data in a multidisciplinary VAC setting, these findings helped clarify syndromic or genetic associations and guide management, including medical therapy, minimally invasive intervention, or surgery. This approach was particularly valuable for venous mapping and intervention planning in patients with anomalous or dilated superficial and/or deep veins, especially when dilated veins connected directly to the deep system (Fig. 2). These patients may require extensive procedures to disconnect enlarged, often incompetent/insufficient veins from the deep veins and prevent life-threatening thromboembolic disease [17].

WB imaging has been used for a range of oncologic and non-oncologic genetic predisposition syndromes [11, 12]. Whole-body contrast-enhanced MRA with gadolinium-based contrast and vessel wall imaging has also been described in Takayasu arteritis [18], and ferumoxytol-based whole-body MRA protocols have been reported in adults [19]. In children, ferumoxytol has been widely used in pediatric populations within the United States over the past decade for indications including congenital heart disease and venous patency mapping [15, 20]. Within vascular anomalies, its use has been reported in hereditary hemorrhagic telangiectasia [21] and pediatric cerebral AVMs [22]. To our knowledge, this is the first use of a WB or limited-WB ferumoxytol-enhanced protocol to evaluate complex, diffuse, or genetically mediated vascular malformations.

Limitations

1. Ferumoxytol is not available in several countries, and its use as a contrast agent is off label. There is also an FDA warning against rapid administration of this agent, which has been associated with life-threatening hypersensitivity reactions. Most centers administer the agent by slow infusion over 15 minutes, with only a fraction of the therapeutic dose required for use as an intravenous contrast agent (diagnostic dose is 2 mg/kg while the therapeutic dose is 8 mg/kg). The safety profile as a diagnostic agent in children using a slow infusion protocol is excellent in large series [14].
2. A localized time-resolved MRA with a separate gadolinium injection may be performed during the same session if a high-flow component is suspected, as small high-flow elements are difficult to exclude by the ferumoxytol protocol alone. Prior review of specialist assessments and targeted ultrasound is therefore important to determine the need and coverage. Although ferumoxytol causes ‘vascular contamination’ of pure arterial imaging, a brisk gadolinium bolus with high-temporal-resolution first-pass acquisition (e.g., TWIST/TRICKS (Time-Resolved Imaging of Contrast KineticS)/keyhole) maintains diagnostic accuracy for high-flow lesions, including in the lungs and extremities.
3. For chest lesions, inversion-recovery 3D-TFE imaging with EKG and respiratory gating may provide superior motion-free images compared with VIBE/RAVE; however, this technique requires specialized expertise and equipment that may not be widely available. Notably, we have found that

3D-RAVE provides diagnostic performance in free-breathing patients even in the chest and abdomen.

4. Our study population did not have adequate representation of PTEN/PHTS patients on the RASopathy spectrum, or those with craniospinal involvement in complex VA. The performance of this protocol in such situations was therefore not adequately assessed and requires further study. Evaluation of brain/spine involvement on large field of view images may be difficult, and subtle findings like small AVMs may be missed without dedicated brain/spine sequences.
5. No imaging reference standard was available due to the nature of this retrospective study. Formal comparison of Ferumoxytol WB MRA to performance of conventional MR sequences in this setting was not performed due to variability of available data.
6. An adjudicated VAC diagnosis after imaging was available in 28/32 patients in the development phase but only 24/45 in the implementation phase, likely reflecting broader WB imaging protocol use across diverse indications (e.g., HHT). Genetic testing was performed in a minority of patients (**Supplement** Table 1), and suspected genetic etiologies may not be confirmed due to limited testing, negative germline results, or inconclusive sampling, which are common challenges with somatic mutations.

Conclusion

In conclusion, we demonstrate feasibility of an abbreviated, whole-body/limited whole-body MR protocol with Ferumoxytol blood-pool contrast for complex vascular anomalies with a genetic predisposition and diffuse involvement. This protocol enables evaluation of fast- and slow-flow lesions and vascular, nonvascular, and organ involvement with strong technical and clinical performance, supports unsupervised use in non-specialized centers, and has shown high acceptance among referral specialists in our experience.

Declarations

Author Contribution

A.L. and R.K. devised and implemented the imaging protocol, trained the imaging team, and supervised data extraction.L.A., R.S., A.L., and R.K. served as expert readers.B.S., E.F., G.P., C.C., A.L., and R.K. participated in multidisciplinary discussions regarding patient management.S.R. collected and analyzed the development-phase data under the supervision of L.A.H.K. collected and analyzed the implementation-phase data under the supervision of R.K.S.R. and H.K. wrote the main manuscript text.A.L. and R.K. contributed to data analysis and manuscript preparation.S.R. and H.K. are joint first authors.A.L. and R.K. are joint senior authors.All authors reviewed the manuscript.

Data Availability

Data generated or analyzed during the study are available from the corresponding author by request.

References

1. Mulliken JB (1982) Classification of pediatric vascular lesions. Plast Reconstr Surg 70(1):120–121
2. Wassef M, Adams BF, Alomari D, Baselga A, Berenstein E, Burrows A, Frieden P, Garzon IJ, Lopez-Gutierrez MC, Lord JC, Mitchel DJ, Powell S, Prendiville J, Vikkula J (2015) ISSVA Board and Scientific Committee. Vascular Anomalies Classification: Recommendations From the International Society for the Study of Vascular Anomalies. Pediatrics 136(1):203–214
3. Moreno-Estébanez A et al (2020) A novel mutation of RASA1 in capillary malformation-arteriovenous malformation syndrome in a case with spinal cord involvement. Clin Neurol Neurosurg 195:105965
4. Choi WK et al (2018) MR-Guided Sclerotherapy for the Treatment of Low-Flow Vascular Malformations. Top Magn Reson Imaging 27(3):153–161
5. Kunimoto KY, Jinnin Y (2022) M, ISSVA Classification of Vascular Anomalies and Molecular Biology. Int J Mol Sci
6. Hussein A, Malguria N (2020) Imaging of Vascular Malformations. Radiol Clin North Am 58(4):815–830
7. Vella M et al (2020) Comparison of MRI, MRA, and DSA for Detection of Cerebral Arteriovenous Malformations in Hereditary Hemorrhagic Telangiectasia. AJNR Am J Neuroradiol 41(6):969–975
8. Yehia L, Eng CPTEN, Hamartoma Tumor S (2001) [Updated 2025 Aug 7]. In: Adam MP, Feldman J, Mirzaa GM, editors. GeneReviews® [Internet]. Seattle (WA): University of Washington, Seattle; 1993–2025. Available from: https://www.ncbi.nlm.nih.gov/books/NBK1488/
9. Kim H, Joh J, Labropoulos N (2022) Characteristics, clinical presentation, and treatment outcomes of venous malformation in the extremities. J Vasc Surg Venous Lymphat Disord 10(1):152–158
10. Sires JD, Williams N, Huilgol SC, Harvey I, Antoniou G, Dawson J (2020) An integrated multidisciplinary team approach to the management of vascular anomalies: challenges and benefits. Pediatr Surg Int 36(10):1149–1156
11. Greer MLC, States LJ, Malkin D, Voss SD, Doria AS (2024) Update on Whole–Body MRI Surveillance for Pediatric Cancer Predisposition Syndromes. Clin Cancer Res 30(22):5021–5033
12. Kraus MS, Yousef AA, Cote SL, Greer MLC (2023) Improving protocols for whole–body magnetic resonance imaging: oncological and inflammatory applications. Pediatr Radiol 53(7):1420–1442
13. Jalili MH, Yu T, Hassani C, Prosper AE, Finn JP, Bedayat A (2022) Contrast-enhanced MR Angiography without Gadolinium-based Contrast Material: Clinical Applications Using Ferumoxytol. Radiol Cardiothorac Imaging 4(4):e210323
14. Nguyen KL, Yoshida T, Kathuria-Prakash N, Zaki IH, Varallyay CG, Semple SI et al (2019) Multicenter Safety and Practice for Off-Label Diagnostic Use of Ferumoxytol in MRI. Radiology 293(3):554–564

15. Dasi A, Kring DN, Selvaraj B, Morgan P, Gerity C, Morgan EE, Krishnamurthy R, Krishnamurthy R (2023) Brand Ferumoxytol vs. generic Ferumoxytol comparison across two dosing regimens: a cardiac MRI image quality study. Pediatr Radiol 53(13):2622–2632
16. Krishnamurthy R, Hernandez A, Kavuk S, Annam A, Pimpalwar S (2015) Imaging the central conducting lymphatics: initial experience with dynamic MR lymphangiography. Radiology 274(3):871–878
17. Reis J 3rd, Alomari AI, Trenor CC 3rd, Adams DM, Fishman SJ, Spencer SA, Shaikh R, Lillis AP, Surnedi MK, Chaudry G (2018) Pulmonary thromboembolic events in patients with congenital lipomatous overgrowth, vascular malformations, epidermal nevi, and spinal/skeletal abnormalities and Klippel-Trénaunay syndrome. J Vasc Surg Venous Lymphat Disord. ;6(4):511–516. 10.1016/j.jvsv.2018.01.015. PMID: 29909856
18. Sun Y, Ma L, Ji Z, Zhang Z, Chen H, Liu H et al (2016) Value of whole–body contrast–enhanced magnetic resonance angiography with vessel wall imaging in quantitative assessment of disease activity and follow–up in Takayasu's arteritis. Clin Rheumatol 35(3):685–693
19. Si G, Liu Y, Sheng J, Ma G, Gao Z, Li Z et al (2025) Exploring Prolonged Efficacy of Ferumoxytol-Enhanced Whole-Body MR Angiography: A Preliminary Study in Healthy Male Subjects. J Magn Reson Imaging 61(3):1515–1518
20. Luhar A, Khan S, Finn JP, Ghahremani S, Griggs R, Zaritsky J, Salusky I, Hall TR (2016) Contrast-enhanced magnetic resonance venography in pediatric patients with chronic kidney disease: initial experience with Ferumoxytol. Pediatr Radiol 46(9):1332–1340
21. Khan SN, McWilliams JP, Bista BB, Kee S, Finn JP (2020) Comparison of Ferumoxytol-enhanced MR Angiography and CT Angiography for the Detection of Pulmonary Arteriovenous Malformations in Hereditary Hemorrhagic Telangiectasia: Initial Results. Radiol Cardiothorac Imaging 2(2):e190077
22. Huang Y, Singer TG, Iv M, Lanzman B, Nair S, Stadler JA, Wang J, Edwards MSB, Grant GA, Cheshier SH, Yeom KW (2019) Ferumoxytol-enhanced MRI for surveillance of pediatric cerebral arteriovenous malformations. J Neurosurg Pediatr 24(4):407–414

Figures

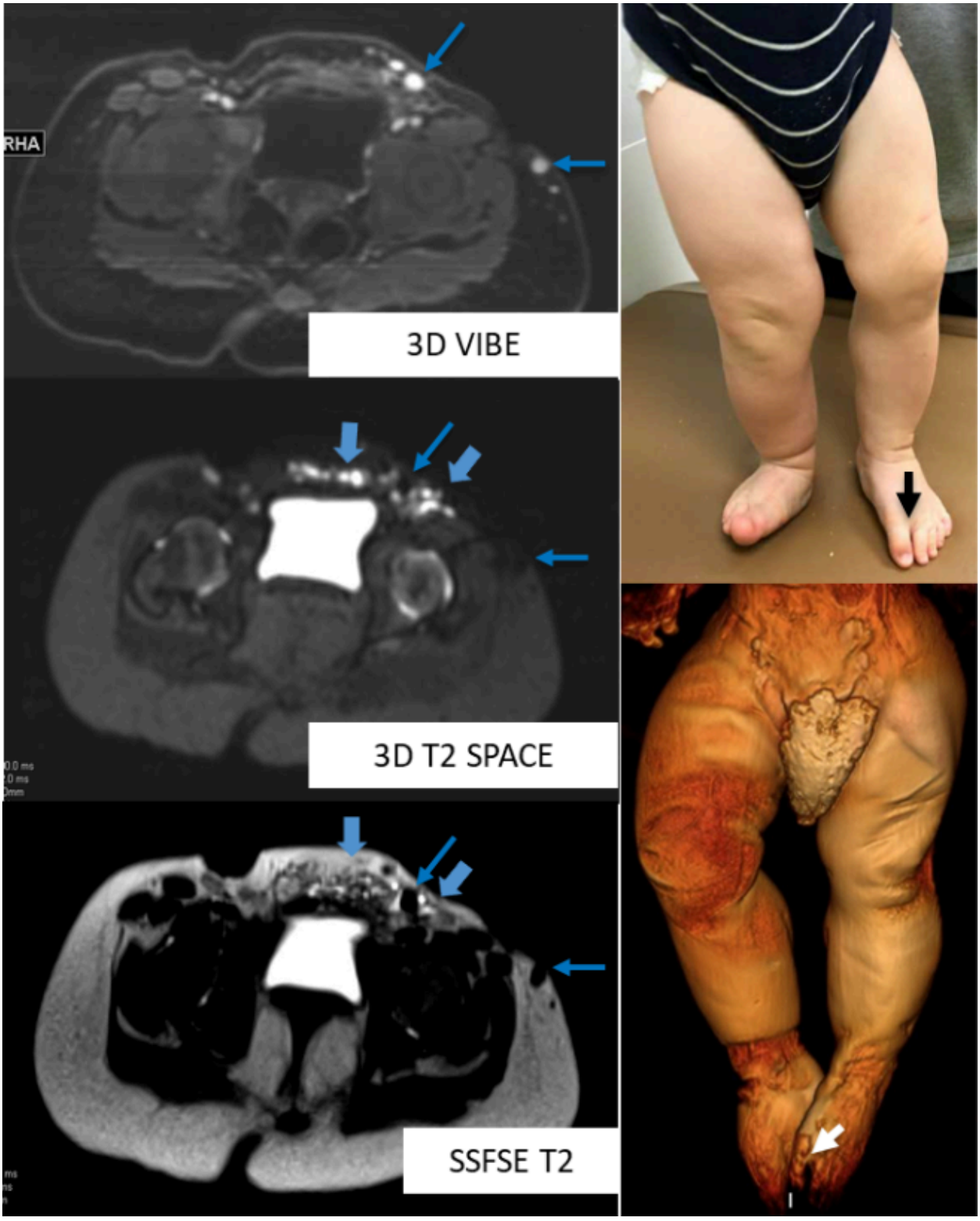


Figure 1

Comparison of core sequences during the evaluation phase:

LEFT column: 18-month-old female with PIK3CA related overgrowth syndrome. 3D VIBE above shows an anomalous vein in the lateral aspect of the left hemipelvis and dilated superficial veins in the left inguinal region (small arrows). Fat suppressed 3D T2 SPACE (middle) and non-fat suppressed 2D SS-FSE T2

below show a microcystic LM in the left inguinal and suprapubic region (large arrows), while the venous and arterial signal is suppressed due to Ferumoxytol (small arrows). 3D T2 SPACE and SSFSE T2 provide redundant information. Lack of fat suppression on SSFSE T2 (bottom) allows improved assessment of fatty involvement compared to 3D T2 SPACE (middle). AVMs were missed on the original diagnosis due to inadequate scan coverage, which was resolved using the new limited WB protocol

RIGHT column: 14-month-old male child with CLOVES syndrome. Comparison of clinical (above) and 3D volume rendered images from a 3D VIBE sequence (below) shows the ability to resolve soft tissue information on the whole-body acquisition showing hemihypertrophy of the right lower extremity and a sandal gap deformity of the left foot (arrow)

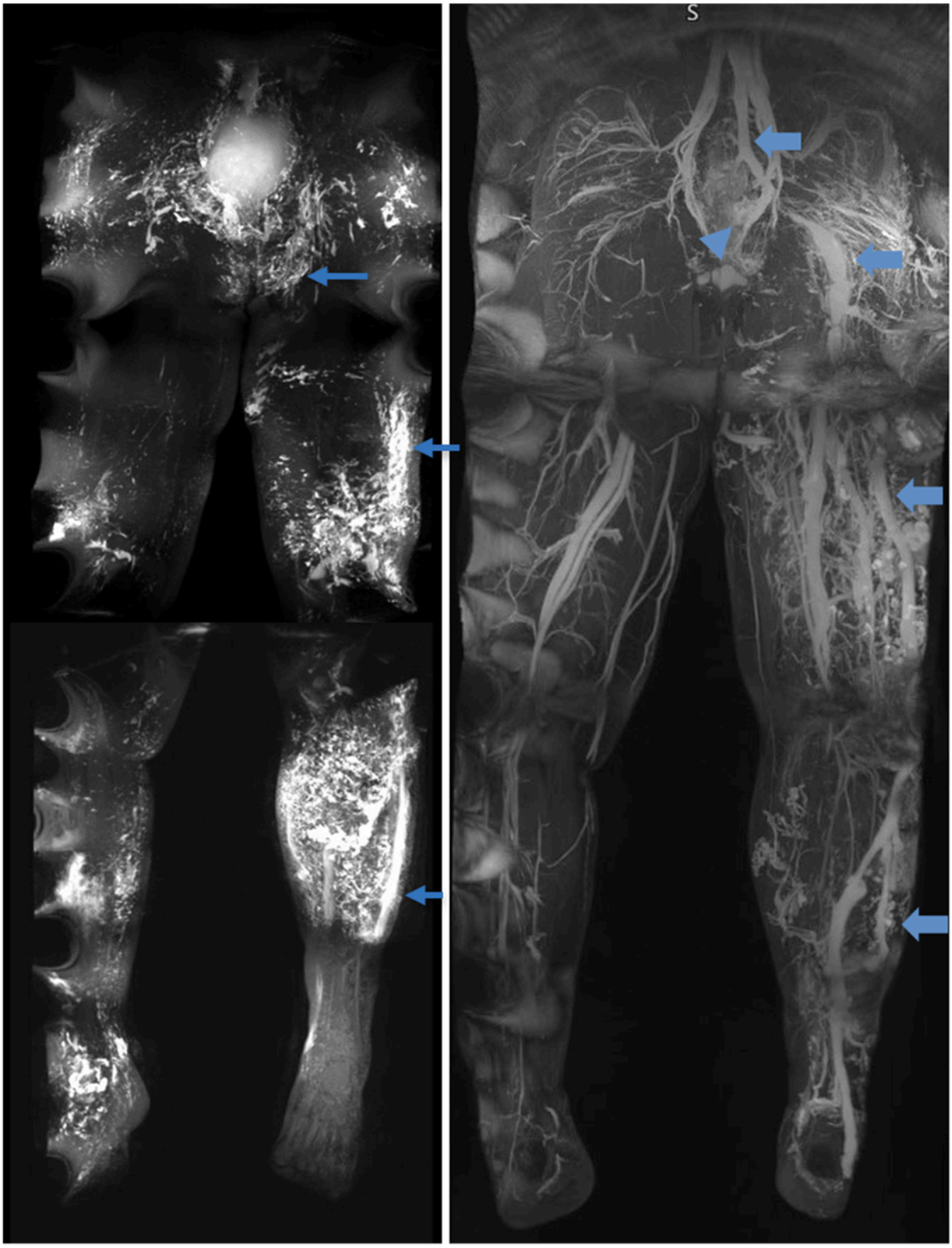


Figure 2

27-year-old male, weighing 132 kg and measuring 187 cm in length with PIK3CA-related overgrowth syndrome (PROS), Klippel-Trenaunay phenotype with overgrowth of the right leg and bilateral feet, and complicated capillary venolymphatic malformation of the left lower extremity and left hemipelvis. Complications included leg length discrepancy, pain, deformity, bleeding per rectum, and secondary infection of lymphatic circumscripta (LM of the skin) in the leg, with previous treatments including

epiphysiodesis for his leg length discrepancy, resection of fatty lesions from his trunk, debulking of the left foot, and sirolimus treatment with significant improvement in quality of life, decreased pain, gradual resolution of leakage from lymphatic circumscripta and improvement of baseline elevated D-dimer. The 2 images illustrate the benefit of this abbreviated protocol in effectively conveying therapeutically relevant information on follow-up. The left image is a composite T2 image showing the distribution of the LM in the perineum, thigh and leg. The right image shows the distribution of venous malformation and anomalous veins including a dominant venous channel along the lateral aspect of the left foot, left leg and left thigh, ultimately draining into an anomalous persistent embryonic sciatic vein and into the internal iliac vein (arrows). The deep veins of the left lower extremity are present and patent. The distribution of the LLE venous malformation is readily seen, including a left perirectal component (blue arrowhead) which was the cause of bleeding per rectum. The transverse dark bands on both images represent the site of stitching of data from separate stations to generate the composite 3D image. The areas of signal dropout on the periphery of the image are artifacts related to the large body habitus of the patient

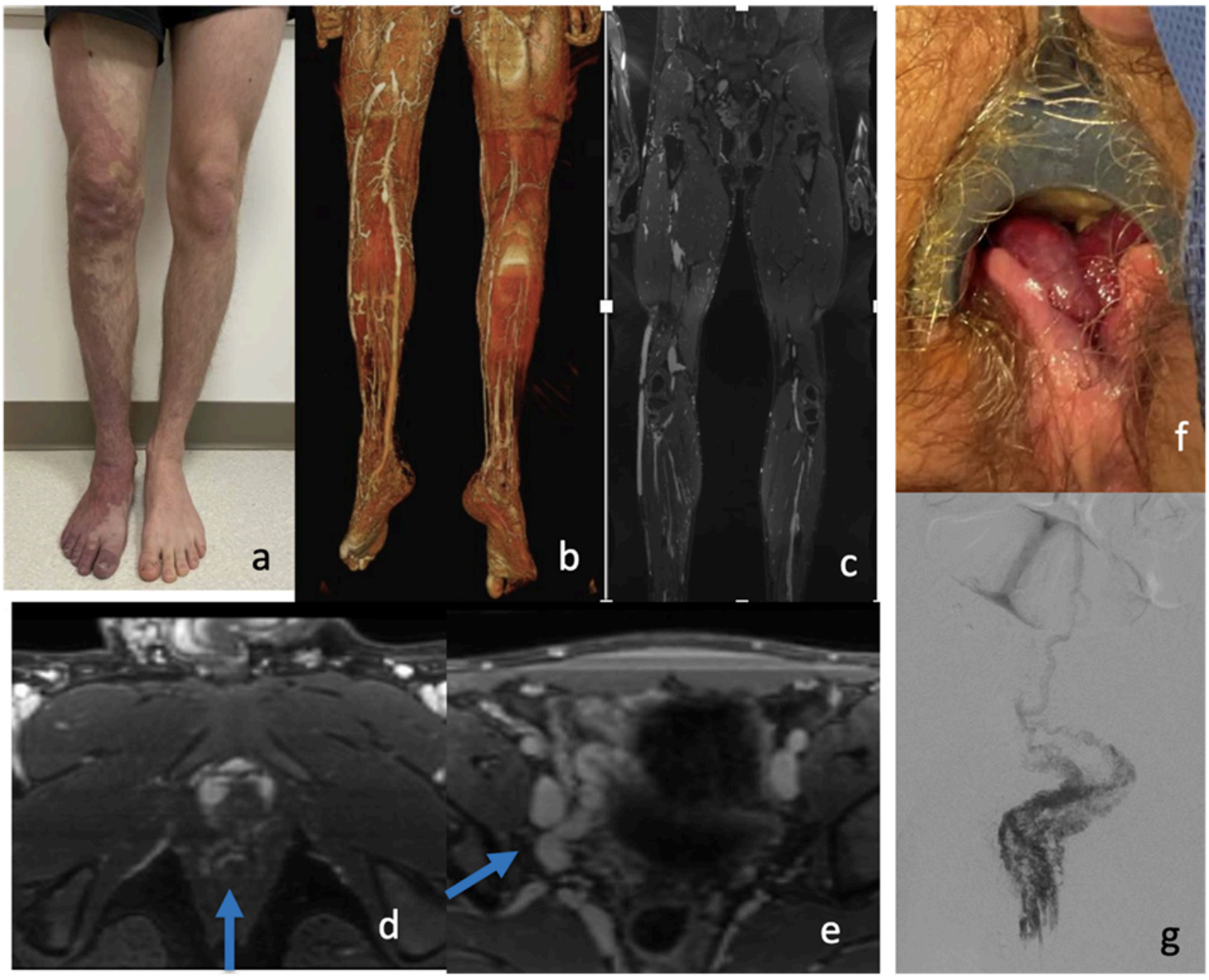


Figure 3

19-year-old male, remote laser therapy for right lower extremity port-wine stain, presenting with intermittent bright red blood per rectum, low hemoglobin requiring blood transfusion

Pre-Imaging Diagnosis: Klippel-Trenaunay Syndrome (KTS)

Post imaging Diagnosis: PIK3CA related Overgrowth Syndrome (PROS) with pelvic/perirectal involvement and anomalous veins with several perforator communications to the intact, but hypoplastic deep veins. A previous conventional MR imaging study of the lower extremity had missed pelvic and peri-rectal involvement, as well as deep vein hypoplasia

Top row shows clinical picture with diffuse port-wine stain (a), 3D volume rendered image (b), and a mid-coronal slice from the WB 3D VIBE sequence (c) showing superficial VM with anomalous vein along the lateral aspect of the right leg, and limb-length discrepancy (LLD)

Bottom row: axial images (d and e) from the 3D VIBE sequence showing submucosal varices in the rectum and anal canal and large perirectal veins in the right hemipelvis (arrows), which were confirmed by proctoscopic evaluation (f) and contrast venography (g) performed prior to successful sclerotherapy

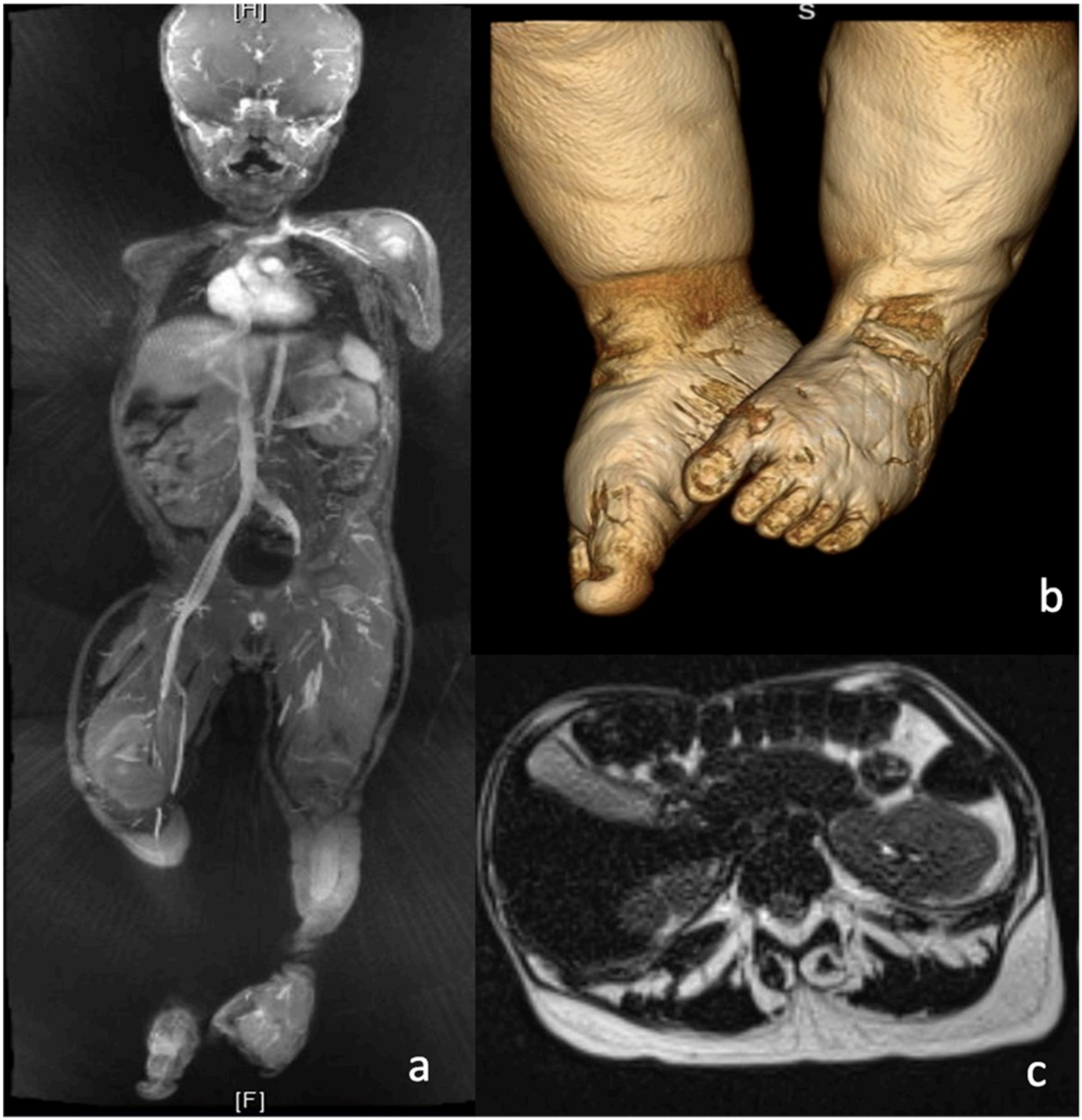


Figure 4

14-month-old male. Pre-procedure and post procedure Dx: CLOVES (Congenital Lipomatous Overgrowth, Vascular malformations, Epidermal nevi, and Spinal/Skeletal anomalies/Scoliosis). A previous conventional MRI/MRA had missed the soft tissue abnormality of the trunk and extremities as well as a diagnosis of CLOVES.

Coronal RAVE image (a) shows normal vascular anatomy with no vascular malformation

3D volume rendering from 3D RAVE (b) shows right lower extremity overgrowth and a left sandal gap deformity of the first and second toes

Axial SSFSE T2 image (c) shows lipomatous overgrowth with fatty infiltration of paraspinal muscles on SSFSE



Figure 5

Use of dual contrast ferumoxytol and gadavist for assessment of suspected high flow component:

38-year-old female, history of right forearm AVM, s/p prior resection and saphenous vein graft to R radial artery in another country, presenting with increasing angulation and pain in the third digit. VAC exam showed focal capillary malformation over upper arm and shoulder (a). Hypervascular lesion affecting the forearm, thumb and third digit (b) with robust color Doppler flow and low-resistance arterial waveforms on spectral Doppler imaging (c). Erosive changes on radiograph of the third digit (d). Limited WB 3D VIBE imaging of the chest and right upper extremity showed dilated tortuous vessels in 3 different locations in the right hand with large draining veins (e and f), and changes related to the saphenous vein graft. No other lesions were noted on WB imaging. Early (g) and late (h) images from a localized time resolved MRA with TWIST with 1.5 second dynamic time of the right hand showed 3 separate AVMs overlying the base of the right first digit, third digit and wrist (arrows). The pre-procedure diagnosis was capillary malformation-arteriovenous malformation. The post-procedure diagnosis was presumed RASopathy, although not confirmed on genetic testing

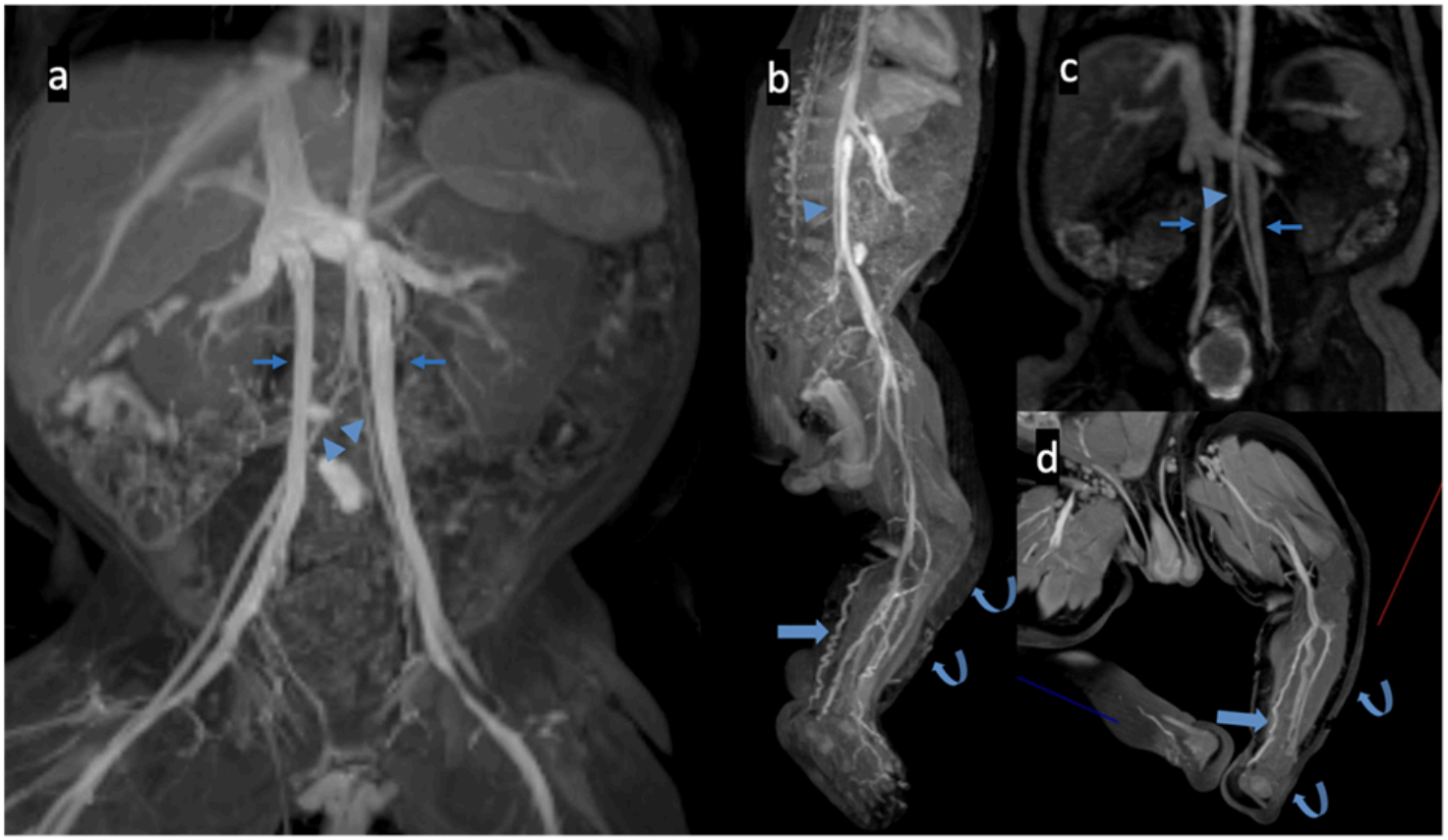


Figure 6

Newborn male with clinical diagnosis of segmental hemangioma of the left lower extremity. The post imaging diagnosis was LUMBAR (Lower body hemangioma, Urogenital abnormalities/ulceration, Myelopathy of the spinal cord, Bony deformities, Anorectal malformations and arterial anomalies, Renal anomalies) syndrome. Images a and b are 3D VIBE and images c and d are from a time resolved MRA using TWIST technique after additional gadolinium administration to screen for a high flow component. There is infrarenal aortic and iliac arterial hypoplasia (arrowheads in a, b and c), duplicated IVC (small arrows in a and c), small saphenous venous dilation and tortuosity in the left lower extremity (large arrows in b and d), and presence of a segmental hemangioma of the left lower extremity (curved arrows in b and d). No arteriovenous shunting was observed

Supplementary Files

This is a list of supplementary files associated with this preprint. Click to download.

- SupplementalFiles.docx